Structure and Reactions of Radicals Derived from Cyclopentane, Cyclopentenes, and Cyclohexenes in Low-Temperature Matrices. An ESR Study

Yoshihiro Kubozono, Makoto Okada, Makoto Aoyagi, Shuichi Yahiro, and Yasuhiko Gondo

Department of Chemistry, Faculty of Science, Kyushu University 33, Hakozaki, Higashiku, Fukuoka 812, Japan

Hiroshi Nakamura and Taku Matsuo

Department of Chemical Science and Technology, Faculty of Engineering, Kyushu University, Hakozaki, Higashiku, Fukuoka 812, Japan

Z. Naturforsch. **46a**, 993–1000 (1991); received August 14, 1991

The radical species derived from cyclopentane, cyclopentenes and cyclohexenes by ^{60}Co γ-ray irradiation at 77 K in halocarbon matrices have been studied by ESR spectroscopy. The electronic and geometrical structures of the radical species are discussed on the basis of the experimental hyperfine coupling constants and semiempirical MO calculations. Exposure of the tetramethylsilane frozen solution containing cyclopentene to ^{60}Co γ-rays produced specifically 3-cyclopenten-1-yl.

1. Introduction

Since the electron beam radiolysis study of neat cyclopentene by Fessenden et al. [1, 2], ESR studies on cyclopentene and cylohexene radical cations in halocarbon matrices have been made by several investigatiors. Shida et al. reported on the structure and reaction of the cyclopentene radical cation in CCl_3F matrix [3]. Lund et al. studied the cyclopentene radical cation in CCl_3CF_3 [4], finding a concentration-dependent reaction [4]. According to these studies [3, 4], the hyperfine coupling (hfc) constants of the two axial and two equatorial β-protons in the cyclopentene radical cation are dependent on the temperature, in contrast to those in the cyclohexene radical cation, and the cyclohexene radical cation is nonplanar in CCl_3F and CCl_3CF_3 at low temperatures.

In the present paper, we report the electronic and geometrical structures and reactions of the radical species derived from cyclopentene and cyclohexene derivatives in low-temperature matrices. Exposure of the cyclopentene and cyclohexene derivatives to ^{60}Co γ-rays in solid matrices resulted in interesting reactions, especially in tetramethylsilane (TMS) matrix. The conformations of the radical species are discussed with the aid of the hfc constants calculated by the UHF-INDO method.

Reprint requests to Prof. Dr. Y. Gondo, Department of Chemistry, Kyushu University 33, Hakozaki, Higashiku, Fukuoka 812, Japan.

2. Experimental

CCl_3CF_3, CCl_2FCClF_2 and TMS (Tokyo Kasei, GR) were used as matrices as received. Cyclopentane, cyclopentene, cyclohexene (Tokyo Kasei, GR), 1-methyl-1-cyclopentene (Aldrich, 98%) and 1-methyl-1-cyclohexene (Wako, 98%) were used as received. Sample solutions of 0.2–1 vol% concentration were fully degassed in suprasil ESR capillary cells, and were irradiated by ^{60}Co γ-ray at 77 K, to a total dose of 0.7 Mrad (1 Mrad = 10^4 J kg^{-1}).

3. Theoretical

The MOPAC Ver. 5.0 available from JCPE [5–8] was used for UHF-AM1 calculations. The GSCF3 [9] and Gaussian 88 programs accessible at the computer center of our institution were used for ab initio calculations. The geometries optimized by use of the single-point UHF-AM1 method under the constraint of specified symmetries G and the accompanying total energies will be referred to as the AM1-G geometries and energies, respectively. The geometries optimized by use of the Gaussian 88 program in UHF mode at the 4-31 G level will be referred to as the G88 geometries. The hfc constants calculated for the AM1-G geometries by use of the UHF-INDO method will be referred to as the INDO-AM1-G hfc constants, while those calculated for the G88 geometries of selected

0932-0784 / 91 / 1100-0993 $ 01.30/0. – Please order a reprint rather than making your own copy.

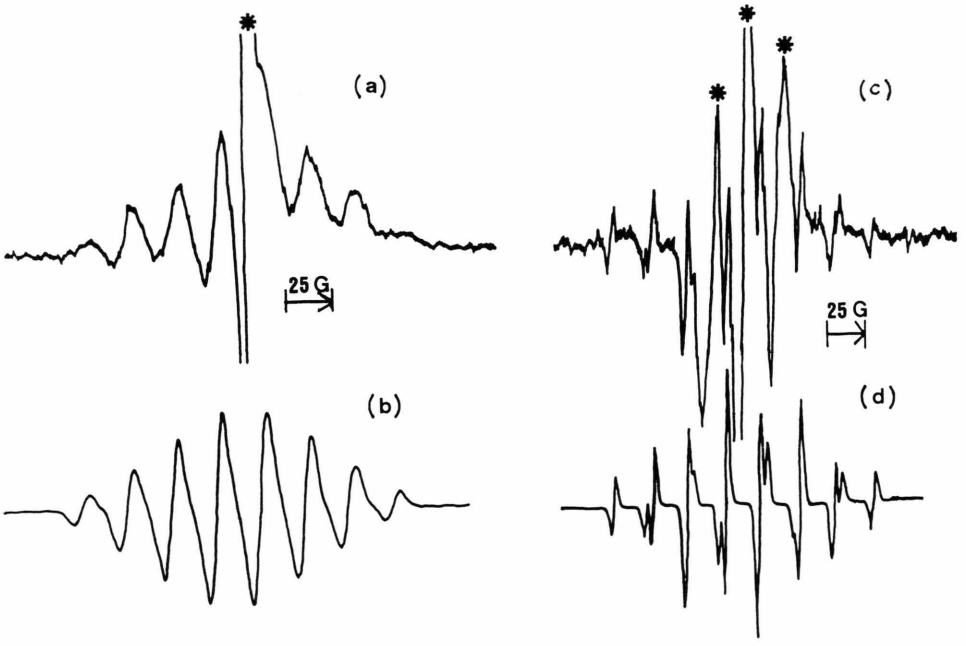

Fig. 1. ESR spectra of cyclopentyl observed in TMS at 77 K (a) and simulated (b), as well as those of 3-cyclopenten-1-yl observed in TMS at 77 K (c) and simulated (d). The simulations are based on the ESR parameters given in text and the Gaussian peak-to-peak line widths $\Delta H = 8.0$ G (b) and 3.0 G (d). The asterisks refer to the signals of the TMS radical and damaged cell.

Table 1. Theoretical ESR parameters.

Radical species		Proton hfc constants/G [a]		
Cyclo-		C_2 geometry ($\varphi' = 25°$)		
pentyl·	(A)	−17.3 (α)	56.6 (β, ax)	29.5 (β, eq)
	(B)	−53.3 (α)	45.9 (β, ax)	26.5 (β, eq)
3-Cyclo-		C_2 geometry ($\varphi' = 30°$)		
penten-1-yl·	(A)	−17.7 (α)	50.3 (β, ax)	24.8 (β, eq)
	(B)	−54.2 (α)	41.8 (β, ax)	24.3 (β, eq)
Cyclo-		C_{2v} geometry		
pentenyl·	(A)	5.2(6)	−12.5(7, 5)	28.3(1, 2, 3, 4)
Cyclo-		C_s geometry ($\varphi = 10°$)		
pentene$^+$·	(C)	−7.0(α)	53.5 (β, ax)	42.5 (β, eq)
		16.1 (γ, ax)	6.5 (γ, eq)	
1-Methyl-		C_s geometry [b] ($\varphi = 10°$)		
1-cyclo-	(C)	−8.6 (α)	50.5 (β5, ax)	40.0 (β5, eq)
pentene$^+$·		37.4 (β2, ax)	29.9 (β2, eq)	
		8.7 (γ, ax)	2.5 (γ, eq)	14.0 (CH_3)
Cyclo-		C_2 geometry ($\varphi' = 30°$)		
hexene$^+$·	(C)	−5.1 (α)	55.4 (β, ax)	24.6 (β, eq)
1-Methyl-		C_2 geometry [b] ($\varphi' = 30°$)		
1-cyclo-	(C)	−8.7 (α)	52.8 (β3, ax)	25.3 (β3, eq)
hexene$^+$·		36.9 (β6, ax)	15.2 (β6, eq)	15.7 (CH_3)

[a] 1 G = 0.1 mT. (A): INDO-AM1; (B): ab initio; (C) INDO. The protons are specified in parentheses. See the theoretical section and relevant inserts.
[b] The stated symmetry does not refer to the substituent.

dihedral or distortion angles, as the case may be, by use of the GSCF3 program in UHF mode at the 4-31 G level will be referred to simply as the ab initio hfc constants. The hfc constants and total energies calculated by use of the UHF-INDO method for assumed, unoptimized geometries of symmetries G will be refered to as the INDO-G hfc constants and energies, respectively. Table 1 and the pertinent figures collect the hfc constants and total energies thus calculated. For comparison, Table 1 also lists the data for the cyclopentene and cyclohexene radical cations which were not studied experimentally in this work.

4. Results and Discussion

4.1. Cyclopentyl

Figure 1 a shows the ESR spectrum of the radical species derived from cyclopentane in TMS at 77 K, which is the same as that of cyclopentyl in CCl_2FCClF_2 at 100 K, converted by deprotonation from the cyclopentane radical cation [10]; the radical species derived from cyclopentane in CCl_2FCClF_2 at 77 K is the

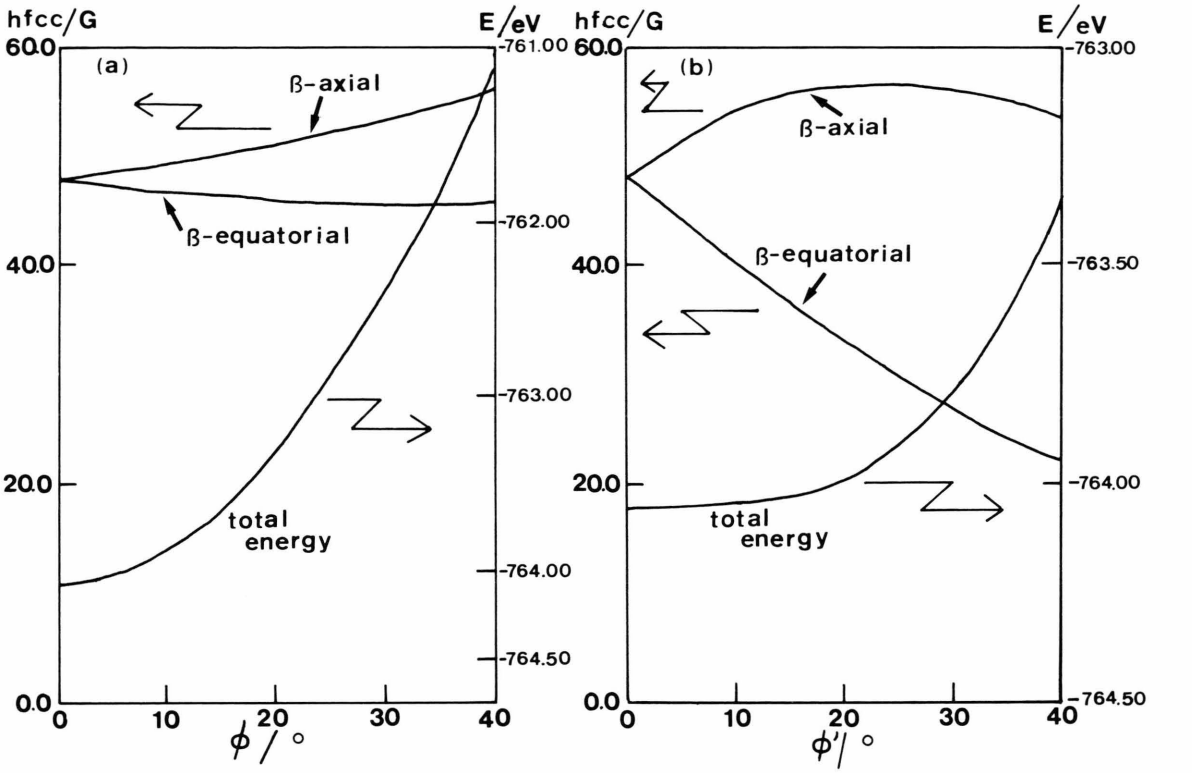

Fig. 2. The dihedral angle dependence of the INDO-AM1-C_s hfc constants (hfcc) for β-protons and AM1-C_s energy (a), and the distortion angle dependence of the INDO-AM1-C_2 hfc constants for the same protons and AM1-C_2 energy (b) of cyclopentyl. See also the theoretical section and the first and second inserts.

cyclopentane radical cation [10]. Figure 1 b shows the spectrum simulated well with the hfc constants of cyclopentyl determined by Lund et al. [10] for α-proton, axial and equatorial β-protons, $a^{H_\alpha}(1\,H) = 21.4$ G (1 G = 0.1 mT), $a^{H_\beta}(ax)(2\,H) = 46.9$ G and $a^{H_\beta}(eq)(2\,H) = 24.4$ G. Thus, it is concluded that ^{60}Co γ-ray irradiation of cyclopentane in TMS at 77 K gives rise to cyclopentyl. The cyclopentyl generated by electron beam radiolysis of neat cyclopentane gives the hfc constants of $a^{H_\alpha}(1\,H) = 21.48$ G and $a^{H_\beta}(4\,H) = 35.16$ G, the hfc constants for β-protons being dynamically averaged [1, 2].

Since we observed the triplet spectrum ascribable to $(CH_3)_3SiCH_2^{\cdot}$ [11, 12], we propose the following reaction scheme for the formation of cyclopentyl in TMS:

$$(CH_3)_4Si + \gamma \rightarrow (CH_3)_4Si^{+\cdot} + e^-,$$

$$(CH_3)_4Si^{+\cdot} + (CH_3)_4Si \rightarrow (CH_3)_4Si^+H + (CH_3)_3SiCH_2^{\cdot},$$

$$(CH_3)_3SiCH_2^{\cdot} + SH \rightarrow S^{\cdot} + (CH_3)_4Si,$$

$$e^- + (CH_3)_4Si^+H \rightarrow (CH_3)_4Si + H^{\cdot},$$

where γ stands for γ-ray and SH is the solute.

Another possible reaction scheme is that the radical cation, $(CH_3)_4Si^{+\cdot}$, directly abstracts a proton from SH to yield $S^{\cdot}$.

The observation of the two distinct hfc constants for the four β-protons, $a^{H_\beta}(ax)$ and $a^{H_\beta}(eq)$, shows that the radical is rigid in TMS matrix at 77 K. This is also contrast to the case of the cyclopentane radical cation in CCl_3CF_3 matrix at 77 K, in which the carbon-ring inversion averages the hfc constants of the four protons on the carbon atoms C_2 and C_5 [13], where the carbon-carbon bonds C_1–C_2 and C_1–C_5 are elongated.

Figure 2 a shows the INDO-AM1-C_s hfc constants for β-protons and AM1-C_s energy, as functions of the dihedral angle φ between the planes of the carbon atoms, C_2–C_1–C_5 and C_2–C_3–C_4–C_5; these hfc constants do not reproduce the experimental in magni-

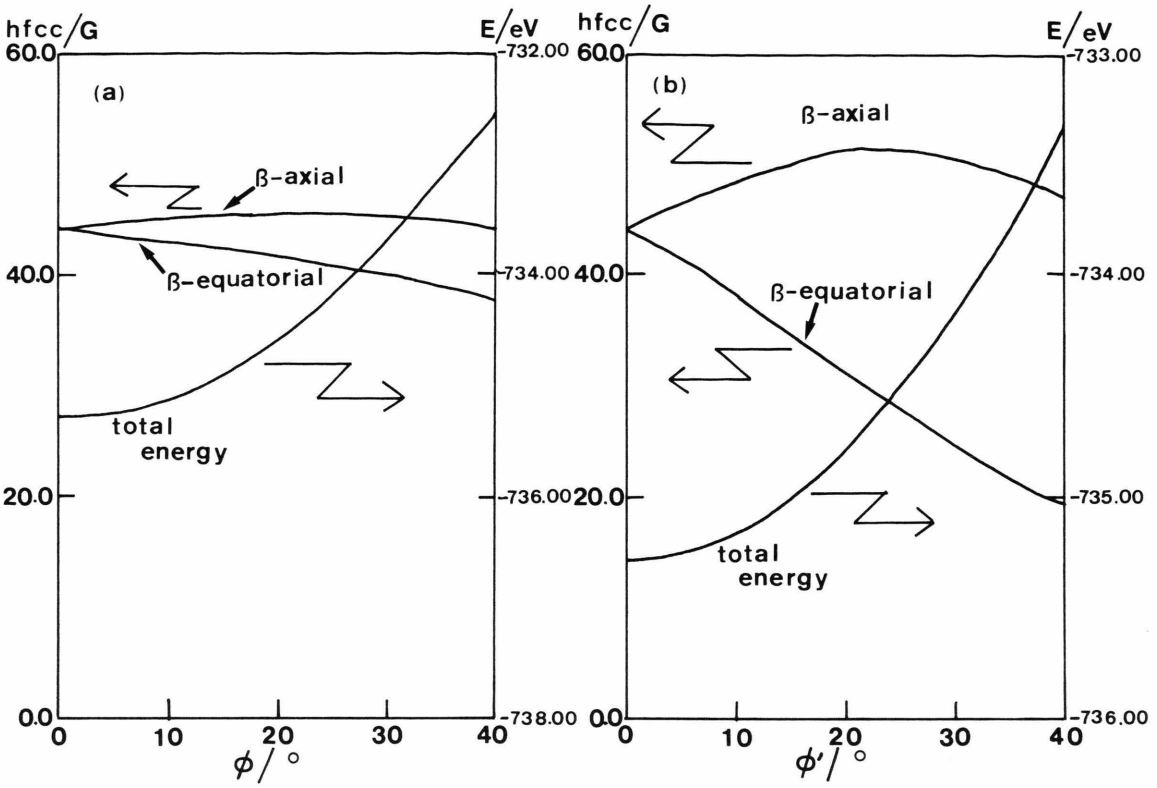

Fig. 3. The dihedral angle dependence of the INDO-AM1-C_s hfc constants (hfcc) for β-protons and AM1-C_s energy (a) and the distortion angle dependence of the INDO-AM1-C_2 hfc constants for the same protons and AM1-C_2 energy (b) of 3-cyclopenten-1-yl. See also the theoretical section and the third and fourth inserts.

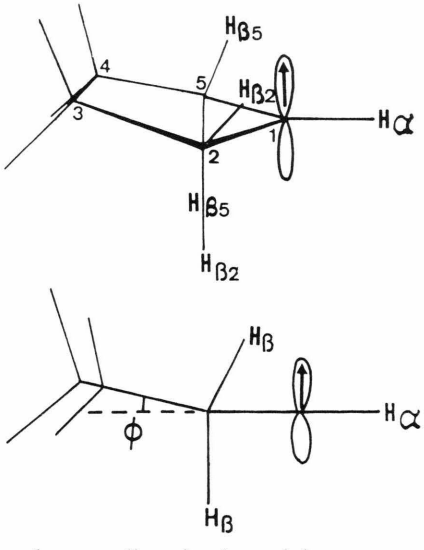

①

tude as well as in the axial-to-equatorial ratio, suggesting that the symmetry of cyclopentyl is different from C_s. Figure 2b shows the INDO-AM1-C_2 hfc constants for β-protons and AM1-C_2 energy, as func-

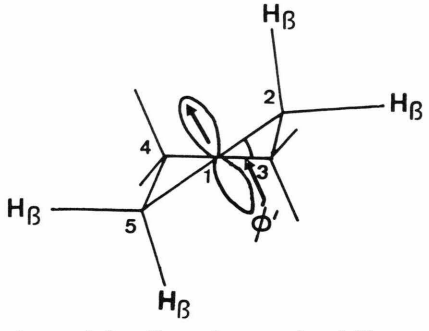

②

tions of the distortion angle φ' illustrated below; the probable φ' value is 25° judging from the axial-to-equatorial ratio, showing that the appropriate symmetry of cyclopentyl is C_2. Thus, Table 1 lists the hfc constants calculated for the C_2 geometries of $\varphi' = 25°$. The listed ab initio hfc constants also reproduce the experimental ones, except for the overestimated absolute value of a^{H_α} as in the case of the methyl radical [14], indicating that cyclopentyl takes C_2 symmetry. According to Lund et al., cyclopentyl is likely to take C_2 symmetry rather than C_s [10].

4.2. 3-Cyclopenten-1-yl

Figure 1c shows the ESR spectrum of the radical species generated from cyclopentene in TMS at 77 K, which differs from that of the cyclopentene radical cation. According to Fessenden et al., cyclopentyl is formed from cyclopentene by addition of a hydrogen atom to α-position and cyclopentyl by hydrogen-atom elimination from β-position [1, 2]. However, the spectrum of Fig. 1c cannot be attributed to any of these radical species. It can be assigned to the 3-cyclopenten-1-yl interpreted to be formed by hydrogen atom elimination from γ-position; as Fig. 1d shows, the spectrum is simulated well with the hfc constants assumed for 3-cyclopenten-1-yl, $a^{H_\alpha}(1\,H) = 20.7$ G, $a^{H_\beta}(ax)(2\,H) = 46.3$ G and $a^{H_\beta}(eq)(2\,H) = 24.7$ G. The γ-proton hfc constants cannot be identified, as is seen from Fig. 1c and Table 1. The similarity of these experimental hfc constants to those of cyclopentyl supports the specific formation of 3-cyclopenten-1-yl in TMS by ^{60}Co γ-ray irradiation, for which the mechanism will be investigated further in a forthcoming paper.

Figure 3a shows the INDO-AM1-C_s hfc constants for β-protons and AM1-C_s energy of 3-cyclopenten-1-yl, as functions of the dihedral angle φ; these hfc constants do not reproduce the experimental, similarly to the case of cyclopentyl. Figure 3b shows the INDO-AM1-C_2 hfc constants for β-protons and AM1-C_2 energy, as functions of the distortion angle φ′; these hfc constants agree well with the observed at around

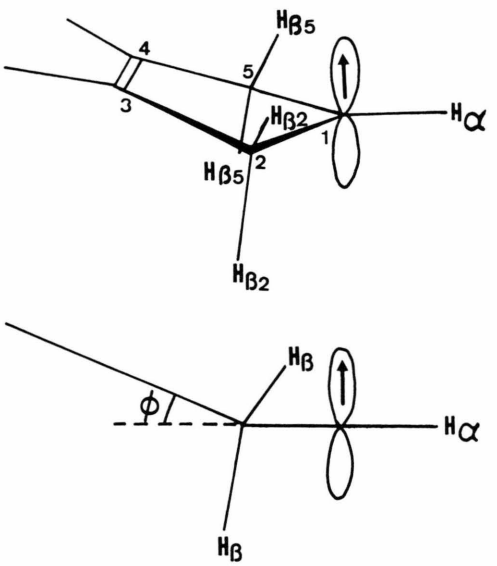

③

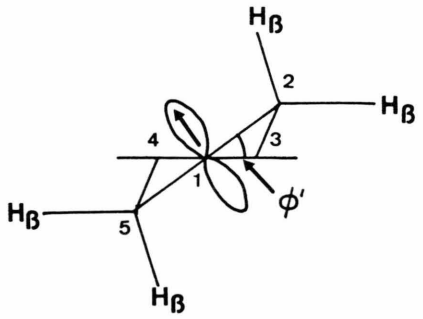

④

$\varphi' = 30°$, although the total energy is not exactly minimal. Thus, Table 1 lists the theoretical hfc constants calculated for the C_2 geometries of $\varphi' = 30°$. The ab initio a^{H_α} is larger in absolute value than the experimental, as in the preceding case of cyclopentyl. As for β-protons, the ab initio hfc constants also well reproduce the experimental. Thus, 3-cyclopenten-1-yl takes C_2 symmetry, similarly to the case of cyclopentyl.

4.3. Cylopentenyl

Figure 4a shows the ESR spectrum observed at 97 K of the radical species derived from cyclopentene in CCl_2FCClF_2. It differs from those of the cyclopentene radical cation in CCl_3F and CCl_3CF_3 reported previously [3, 4], while it is the same as that observed at 155 K of the allylic radical in CCl_3F formed through cation-parent molecule reaction [3], and is also the same as that of cyclopentenyl [1, 2].

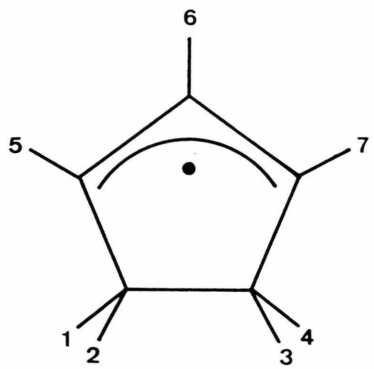

⑤

Figure 4b shows the spectrum simulated well with $a^{H_{1,2,3,4}}(4\,H) = 23.4$ G, $a^{H_{5,7}}(2\,H) = 14.4$ G and $a^{H_6}(1\,H) = 3.1$ G. These hfc constants are similar to those of cyclopentenyl in CCl_3F [3], but a little different from those in neat cyclopentene, $a^{H_{1,2,3,4}}(4\,H) = 19.75$ G, $a^{H_{5,7}}(2\,H) = 15.50$ G and $a^{H_6}(1\,H) = 2.76$ G [1, 2]. The discrepancies may be due to the difference in matrix.

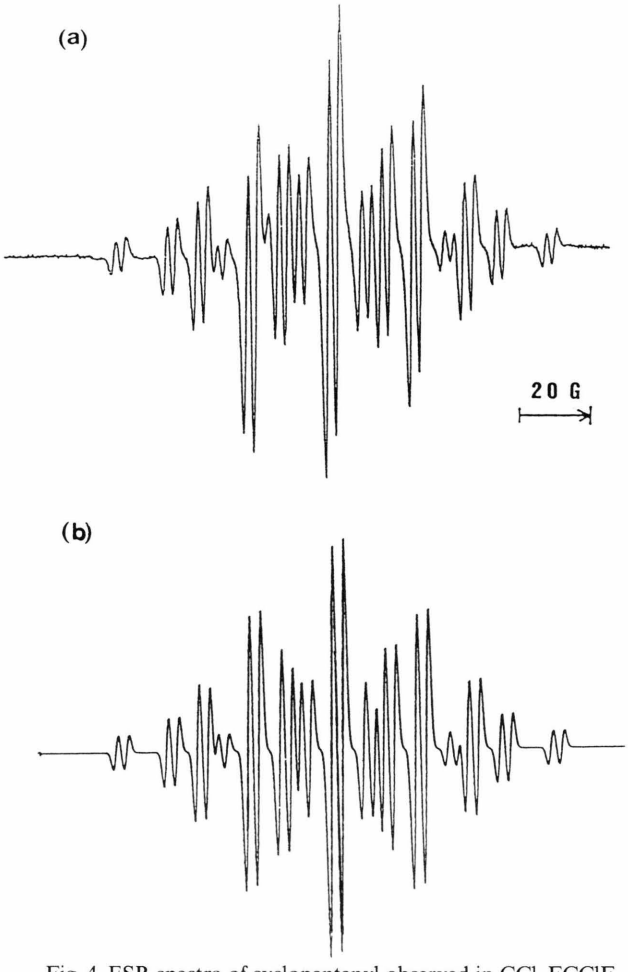

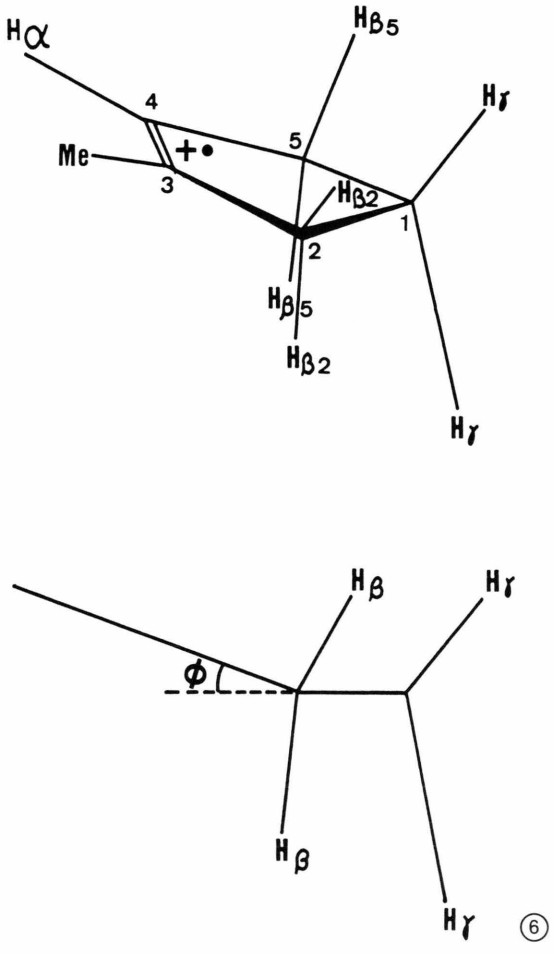

Fig. 4. ESR spectra of cyclopentenyl observed in CCl_2FCClF_2 at 97 K (a) and simulated (b). The simulation is as in Fig. 1, except for the width $\Delta H = 1.5$ G.

The INDO-AM1-C_{2v} hfc constants listed in Table 1 well reproduce the experimental, confirming the formation of cyclopentenyl.

In CCl_2FCClF_2, the allylic radical is formed even at 77 K.

4.4. 1-Methyl-1-cyclopentene Radical Cation

Figure 5a shows the ESR spectrum of 1-methyl-1-cyclopentene radical cation in CCl_3CF_3 observed at 133 K. Figure 5b shows the spectrum simulated well with $a^{H_\alpha}(1\,H) = 11.8$ G, $a^{CH_3}(3\,H) = 17.7$ G, $a^{H_{\beta 5}}(2\,H) = 48.4$ G of β-protons nonadjacent to the methyl group, $a^{H_{\beta 2}}(2\,H) = 36.0$ G of β-protons adjacent to the methyl group, and $a^{H_\gamma}(2\,H) = 3.6$ G. The methyl group rotates freely as indicated by the methyl-proton isotropic four lines. The electronic structure is affected remarkably by the methyl group, as $a^{H_{\beta 2}}$ is considerably different from $a^{H_{\beta 5}}$. The 1-methyl-1-cyclopentene radical cation exerts a rapid puckering motion at 133 K in the same manner as the cyclopentene radical cation, since the above values of β- and γ-protons are the averaged ones.

Table 1 collects the INDO-C_s hfc constants of the cyclopentene and 1-methyl-1-cyclopentene radical cations calculated with the carbon skeleton of cyclopentene with C_s-symmetry [15] and the dihedral angle $\varphi = 10°$ of the cyclopentene radical cation [3]; these hfc constants are in good agreement with the observed, particularly those for β-protons nonadjacent to the methyl group being larger than those for β-protons adjacent. The 1-methyl-1-cyclopentene radical cation is concluded to take $\varphi \cong 10°$, showing little effect of the methyl group on the molecular structure.

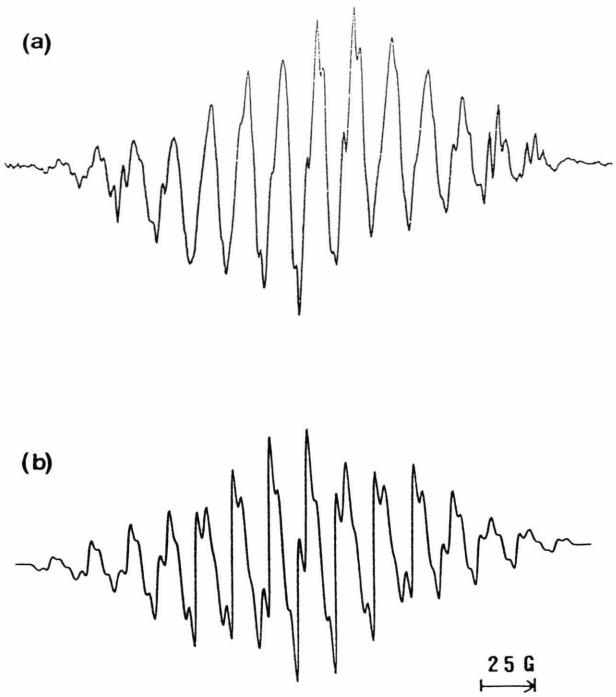

Fig. 5. ESR spectra of the 1-methyl-1-cyclopentene radical cation in CCl_3CF_3 observed at 133 K (a) and simulated (b). The simulation is as in Fig. 1, except for the width $\Delta H =$ 3.4 G.

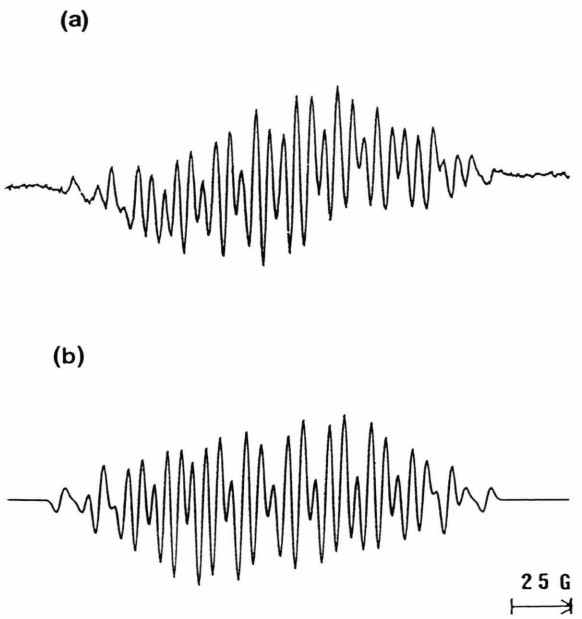

Fig. 6. ESR spectra of the 1-methyl-1-cyclohexene radical cation in CCl_3CF_3 observed at 133 K (a) and simulated (b). The simulation is as in Fig. 1, except for the width $\Delta H =$ 3.9 G.

4.5. 1-Methyl-1-cyclohexene Radical Cation

Figure 6a shows the ESR spectrum of the 1-methyl-1-cyclohexene radical cation in CCl_3CF_3 observed at 133 K. Figure 6b shows the spectrum simulated well with $a^{H_\alpha}(1H) = 11.6$ G, $a^{CH_3}(3H) = 17.9$ G, $a^{H_{\beta 3}}(ax)(1H) = 38.7$ G and $a^{H_{\beta 3}}(eq)(1H) = 30.4$ G of axial and equatorial β-protons nonadjacent to the methyl group, and $a^{H_{\beta 6}}(ax)(1H) = 36.2$ G and $a^{H_{\beta 6}}(eq)(1H) = 24.5$ G of axial and equatorial β-protons adjacent to the methyl group. The hfc constants of the axial and

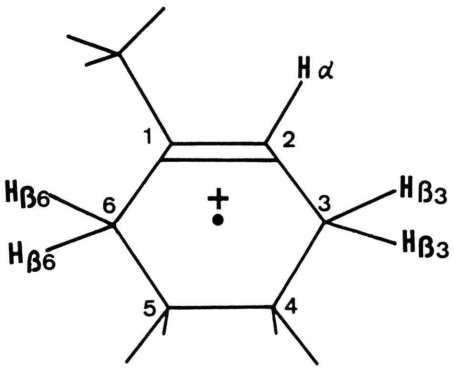

⑦

equatorial β-protons are distinct in the 1-methyl-1-cyclohexene radical cation as in the cyclohexene radical cation [3, 4], indicating that the cyclohexene and 1-methyl-1-cyclohexene radical cations are rigid in structure even at 133 K. The methyl group rotation is free similarly to the case of the 1-methyl-1-cyclopentene radical cation. The hfc constants for β-protons nonadjacent to the methyl group are fairly larger than those for the other β-protons.

Figures 7a and b show the INDO-C_2 hfc constants of β-protons and INDO-C_2 energies of the cyclohexene and 1-methyl-1-cyclohexene radical cations, respectively, as functions of the distortion angle φ' defined below, calculated by use of the half-chair carbon skeleton of cyclohexene with C_2-symmetry [16].

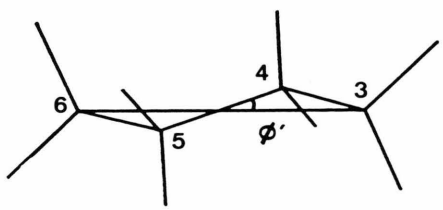

⑧

The total energy is minimal at around $\varphi' = 30°$, either for the cyclohexene or for the 1-methyl-1-cyclohexene radical cation. When $\varphi' = 25° - 30°$, the INDO-C_2 hfc constants of the cyclohexene radical cation are in

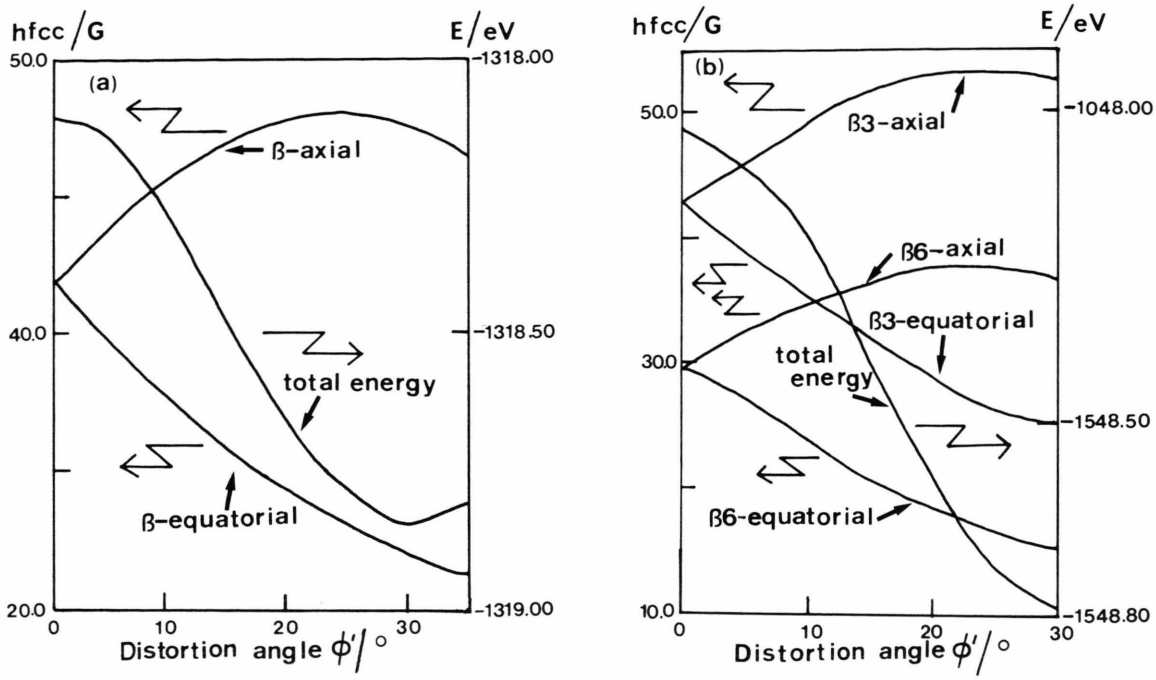

Fig. 7. The distortion angle dependences of the INDO-C_2 hfc constants (hfcc) for β-protons and INDO-C_2 energies of the cyclohexene radical cation (a), and 1-methyl-1-cyclohexene radical cation (b). See the theoretical section and the seventh and eighth inserts.

good agreement with the observed, as Fig. 7a shows. The φ' range is also reasonable from the INDO-C_2 energy. The cyclohexene radical cation is similar in geometry to cyclohexene for which $\varphi' \cong 30°$ [16]. As for the 1-methyl-1-cyclohexene radical cation, the INDO-C_2 hfc constants are in qualitative agreement with the observed, overestimating for the axial β-protons and underestimating for the equatorial β-protons, as Fig. 7b shows.

Table 1 collects the INDO-C_2 hfc constants for the cyclohexene and 1-methyl-1-cyclohexene radical cations with $\varphi' = 30°$, which are in good agreement with the observed for the former cation, but are in qualitative agreement for the latter. The observed hfc constants of β-protons nonadjacent to the methyl group are larger than those of the other β-protons, as the theory also predicts, reflecting the electron-donating nature of the methyl group.

The authors wish to thank Messrs. Hiroki Ujita and Tatsuya Miyamoto for their helpful assistance. All MO calculations were carried out on a Facom M-780/20 system at the Computer Center of Kyushu University.

[1] R. W. Fessenden and R. H. Schuler, J. Chem. Phys. **39,** 2147 (1963).
[2] R. W. Fessenden and R. H. Schuler, in: Advances in Radiation Chemistry, Vol. 2 (M. Burton and J. L. Magee, eds.), Wiley-Interscience, New York 1969, p. 1.
[3] T. Shida, Y. Egawa, H. Kubodera, and T. Kato, J. Chem. Phys. **73,** 5963 (1980).
[4] M. Tabata and A. Lund, Chem. Phys. **75,** 379 (1983).
[5] M. J. S. Dewar and W. Thiel, J. Amer. Chem. Soc. **99,** 4899 (1977).
[6] M. J. S. Dewar, E. G. Zoebisch, E. F. Healy, and J. J. P. Stewart, J. Amer. Chem. Soc. **107,** 3902 (1985).
[7] J. J. P. Stewart, QCPE Bull. **9,** 10 (1989).
[8] T. Hirano, JCPE Newsletter **1,** 10 (1989).
[9] N. Kosugi, Theor. Chim. Acta **72,** 149 (1987).
[10] L. Sjöqvist, M. Lindgren, and A. Lund, Chem. Phys. Lett. **156,** 323 (1989).
[11] J. H. Mackey and D. E. Wood, Mol. Phys. **18,** 783 (1970).
[12] R. V. Lloyd, J. Phys. Chem. **83,** 276 (1979).
[13] L. Sjöqvist, A. Lund, and J. Maruani, Chem. Phys. **125,** 293 (1988).
[14] A. Szabo and N. S. Ostlund, Modern Quantum Chemistry, McGraw-Hill, New York 1989, p. 216.
[15] M. I. Davis and T. W. Muecke, J. Phys. Chem. **74,** 1104 (1970).
[16] J. F. Chiang and S. H. Bauer, J. Amer. Chem. Soc. **91,** 1898 (1969).